News on PHOTOS Monte Carlo: $\gamma^* \to \pi^+\pi^-(\gamma)$ and $K^\pm \to \pi^+\pi^- e^\pm \nu(\gamma)$ *

XU Qing-Jun(徐庆君)[1;1]   Z. Wąs[1,2;2]

[1] Institute of Nuclear Physics, PAN, Kraków, ul. Radzikowskiego 152, Poland
[2] CERN PH-TH, CH-1211 Geneva 23, Switzerland

Abstract PHOTOS Monte Carlo is widely used for simulating QED effects in decay of intermediate particles and resonances. It can be easily connected to other main process generators. In this paper we consider decaying processes $\gamma^* \to \pi^+\pi^-(\gamma)$ and $K^\pm \to \pi^+\pi^- e^\pm \nu$ (γ) in the framework of Scalar QED. These two processes are interesting not only for the technical aspect of PHOTOS Monte Carlo, but also for precision measurement of $\alpha_{\mathrm{QED}}(M_Z)$, $g-2$, as well as $\pi\pi$ scattering lengths.

Key words Monte Carlo generator, QED radiative corrections, K_{e4} decay

PACS 13.40.Ks, 13.66.Bc, 13.20.Eb

1 Introduction

In high energy experiments, one of the crucial works is to compare new experiment results with predictions from the theory. If the agreement is obtained, the theory is proved to be true. Otherwise one may think that the theory calculations turned out to be wrong or the effect of new physics appeared. Monte Carlo generators, rather than analytical calculations, are required to provide theoretical results of real experiment interest. The PHOTOS Monte Carlo [1, 2] is a universal Monte Carlo algorithm that is designed for simulating QED radiative corrections in cascade decays. It is widely used in low energy experiments and high energy experiments as well. The program is based on exact multiphoton phase space while the matrix element is approximately taken as process independent multidimensional kernel. In some cases, the exact first order matrix element is employed in order to improve the precision.

From the experience gained in KKMC project [3, 4] where spin amplitudes were used, one concludes that spin amplitudes are essential for design and tests of the program, in particular for choice of the single emission kernels. The analysis of the spin amplitudes

and tests for the algorithm in case of Z decay into pair of charged fermion was given in Ref. [5]. The case of the scalar particle decay into pair of fermions is covered in Ref. [6] and the decay of spinless particle into pair of scalars is studied in Ref. [7]. The case of W decay was covered in Ref. [8, 9].

In this paper we will study spin amplitudes for $\gamma^* \to \pi^+\pi^-(\gamma)$ decay. It not only provides example for studies of Lorentz and gauge group properties of spin amplitudes and cross sections, but also is important to improve theoretical uncertainty of PHOTOS for this decay. Furthermore, it is of great experiment interest since its relevance to precision measurement of $\alpha_{\mathrm{QED}}(M_Z)$ and $g-2$.

K_{e4} decay could give the unique information on the value of $s-$ and $p-$ wave $\pi\pi$ scattering lengths. The high statistics measurements of K_{e4} decay has been performed by NA48/2 collaboration at CERN [10]. Theoretical predictions are well calculated [11] and the difference between theoretical prediction and experiment value is about 7%. In particular, QED corrections to this process are known to be nonnegligible. They need to be taken into account with the help of Monte Carlo because their size depend on detector acceptance. In NA48 experiment, to take

into account QED effects, PHOTOS Monte Carlo is used together with Coulomb correction (see Ref. [10]). In this paper we consider QED radiative corrections to K_{e4} decay and implement it into PHOTOS Monte Carlo.

The paper is organized as follows: process $\gamma^* \to \pi^+\pi^-(\gamma)$ is studied in Section 2, Section 3 will come to K_{e4} decay, summary will be in Section 4.

2　$\gamma^* \to \pi^+\pi^-(\gamma)$

In order to match the parton shower and the hard bremsstrahlung matrix element into interference weight, the matrix element of $\gamma^* \to \pi^+\pi^-(\gamma)$ needs to be studied in great detail. Its gauge invariant parts need to be identified and relations to amplitudes of lower orders have to be found.

2.1　Spin amplitude

Consider the process $e^+e^- \to \gamma^*(p) \to \pi^+(q_1)\pi^-(q_2)\gamma(k,\epsilon)$, see Fig. 1.
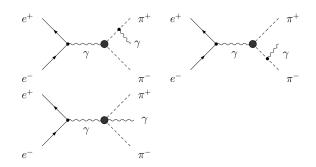

Fig. 1.　Feynman diagrams of $e^+e^- \to \gamma^* \to \pi^+\pi^-\gamma$

The amplitudes equivalent to those given in Ref. [12] are obtained. It can be written as

$$M = V^\mu H_\mu, \qquad (1)$$

where $V_\mu = \bar{v}(p_1,\lambda_1)\gamma_\mu u(p_2,\lambda_2)$. The $p_1,\lambda_1,p_2,\lambda_2$ are momenta and helicities of the incoming electron and positron. V_μ defines the spin state of the intermediate γ^*.

Let us focus on the part for virtual photon decay. Following conventions of Ref. [12], the final interaction part of the Born matrix element for such process is

$$H_0^\mu(p,q_1,q_2) = \frac{eF_{2\pi}(p^2)}{p^2}(q_1-q_2)^\mu. \qquad (2)$$

Here $p = q_1+q_2$. If photon is present, this part of the amplitude reads:

$$H^\mu = \frac{e^2 F_{2\pi}(p^2)}{p^2}\left\{(q_1+k-q_2)^\mu \frac{q_1\cdot\epsilon^*}{q_1\cdot k}+\right.$$

$$\left. (q_2+k-q_1)^\mu \frac{q_2\cdot\epsilon^*}{q_2\cdot k} - 2\epsilon^{*\mu}\right\}. \qquad (3)$$

It makes sense to rewrite Eq. (3) explicitly as sum of two gauge invariant terms:

$$H^\mu = H_{\mathrm{I}}^\mu + H_{\mathrm{II}}^\mu, \qquad (4)$$

$$H_{\mathrm{I}}^\mu = \frac{e^2 F_{2\pi}(p^2)}{p^2}\left((q_1-q_2)^\mu + k^\mu \frac{q_2\cdot k - q_1\cdot k}{q_2\cdot k + q_1\cdot k}\right)\times$$

$$\left(\frac{q_1\cdot\epsilon^*}{q_1\cdot k} - \frac{q_2\cdot\epsilon^*}{q_2\cdot k}\right), \qquad (5)$$

$$H_{\mathrm{II}}^\mu = \frac{2e^2 F_{2\pi}(p^2)}{p^2}\left(\frac{k^\mu(q_1\cdot\epsilon^* + q_2\cdot\epsilon^*)}{q_2\cdot k + q_1\cdot k} - \epsilon^{*\mu}\right). \qquad (6)$$

One can easily see that Eq. (5) has a typical form for amplitudes of QED exclusive exponentiation [13], that is Born-like -expression multiplied by an eikonal factor

$$\left(\frac{q_1\cdot\epsilon^*}{q_1\cdot k} - \frac{q_2\cdot\epsilon^*}{q_2\cdot k}\right).$$

The expression in front of the factor indeed approaches the Born one in soft photon and collinear photon limit. Thus, it is consistent with LL level factorization into Born amplitude and eikonal factor.

If One takes separation (4) for the calculation of two parts of spin amplitudes, then after spin average, the expression for the cross section takes the form:

$$\sum_{\lambda,\epsilon}|M|^2 = \sum_{\lambda,\epsilon}|M_{\mathrm{I}}|^2 + \sum_{\lambda,\epsilon}|M_{\mathrm{II}}|^2 + 2\sum_{\lambda,\epsilon}M_{\mathrm{I}}M_{\mathrm{II}}^*. \qquad (7)$$

We should stress that Eq. (7) can have its first term even closer to Born-times-eikonal-factor form. For that purpose it is enough to adjust normalization of the first part of Eq. (7) to Born amplitude times eikonal factor, and replace $|M_{\mathrm{I}}|^2$ with

$$|M_{\mathrm{I}}'|^2 = |M_{\mathrm{I}}|^2 \frac{|\vec{q_1}-\vec{q_2}|^2_{\mathrm{Born}}}{|\vec{q_1}-\vec{q_2}+\vec{k}\frac{q_2\cdot k - q_1\cdot k}{q_2\cdot k + q_1\cdot k}|^2}. \qquad (8)$$

Compensating adjustment to the remaining parts of Eq. (7) is then necessary. Since $\sum_{\lambda,\epsilon}|M_{\mathrm{I}}'|^2$ is the expression used in PHOTOS Monte Carlo in Ref. [7], such a modification is of interest. In the next section, we will perform our numerical investigations with respect to Ref. [7] which is a reference for us.

2.2 Numerical results

We will show results at 2 GeV center of mass energy. Comparison of result from $\sum_{\lambda,\epsilon} |M'_\mathrm{I}|^2$ with result from PHOTOS with matrix element taken from Ref. [7] is shown in Fig. 2. One can see that agreement is excellent all over the phase space. It is true only for the case when distributions are averaged over the orientation of the whole event with respect to incoming beams (or spin state of the virtual photon).

If instead of $\sum_{\lambda,\epsilon} |M'_\mathrm{I}|^2$ one would use directly $\sum_{\lambda,\epsilon} |M_\mathrm{I}|^2$, that is when normalization of Born-like factor is not performed, difference with respect to formulas in Ref. [7] is much larger, see Fig. 3.
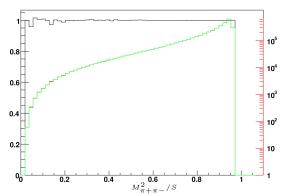

Fig. 2.   Comparison of result using $\sum_{\lambda,\epsilon} |M'_\mathrm{I}|^2$ (green line) with that using matrix element taken from Ref. [7] (red line). Black line represents their ratio.
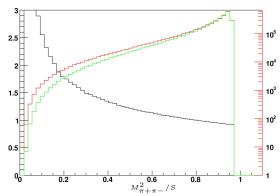

Fig. 3.   Comparison of result using $\sum_{\lambda,\epsilon} |M_\mathrm{I}|^2$ (green line) with that using matrix element taken from Ref. [7] (red line). Black line represents their ratio.

Finally let us compare result of complete scalar QED matrix element with that of matrix element taken from Ref. [7], see Fig. 4. At high photon energy region, there is clear surplus of events with respect to formula in Ref. [7]. That contribution should not be understood as bremsstrahlung, but rather as genuine process. Anyway in that region of phase space

scalar QED is not expected to work well. Note that the difference between results of Figs. 2 and 4 is only 0.2% of the total process rate. That is why our detailed discussion is not important for numerical conclusions, but important for understanding the underlying structure.

From Fig. 2 one could conclude that the universal kernel in Ref. [7], for arbitrary large samples, is equivalent to the matrix element $\sum_{\lambda,\epsilon} |M'_\mathrm{I}|^2$. But differences appear in distributions sensitive to initial state spin orientation, see Figs. 5 and 6. On these
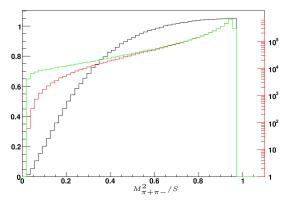

Fig. 4.   Comparison of result using complete matrix element (green line) with that using matrix element taken from Ref. [7] (red line). Black line represents their ratio.
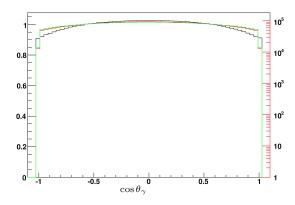

Fig. 5.   Comparison of result using $\sum_{\lambda,\epsilon} |M'_\mathrm{I}|^2$ (green line) with that using matrix element taken from Ref. [7] (red line). Black line represents their ratio.

plots angular distributions of the photon momentum and π^+ momentum with respect to the beam line are shown, respectively. Regions of phase space giving near zero contribution at the Born level are becoming more populated if approximation for the photon radiation matrix element [7] is used.
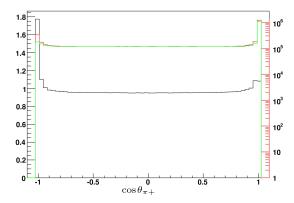
Fig. 6. Comparison of result using $\sum_{\lambda,\epsilon} |M'_{\mathrm{I}}|^2$ (green line) with that using matrix element taken from Ref. [7] (red line). Black line represents their ratio.

3 $\mathbf{K^\pm \to \pi^+\pi^- e^\pm \nu(\gamma)}$

In this section radiative corrections to K_{e4} decay are calculated following approximations explained in Ref. [14]. We compare it with Coulomb corrections used by NA48/2 collaboration. The hard photon bremsstruhlung is calculated analytically with soft photon and collinear photon approximation. Numerical tests with PHOTOS Monte Carlo are performed.

3.1   QED radiative corrections to $K_{\mathbf{e4}}$ decay

Consider K_{e4} decay,

$$\mathrm{K}^\pm(p) \to \pi^+(q_+) + \pi^-(q_-) + \mathrm{e}^\pm(p_e) + \nu(p_\nu). \quad (9)$$

In the framework of Scalar QED but neglecting diagrams with photons emission from hadronic or weak blocks, one can calculate the virtual photon corrections. Note that the electron photon vertex is taken from standard QED. Contribution of virtual diagrams reads

$$\frac{\mathrm{d}\Gamma_{\mathrm{virt}}}{\mathrm{d}\Gamma_{\mathrm{Born}}} = \frac{\alpha}{\pi}\left[\ln\frac{m}{\lambda}\left(4 + \frac{L_-}{\beta_-} - \frac{L_+}{\beta_+} - 2\rho - \frac{1+\beta^2}{\beta}L_\beta + \right.\right.$$

$$2\ln\frac{p_e \cdot q_+}{p_e \cdot q_-}\right) + \pi^2\frac{1+\beta^2}{2\beta} + \rho^2 + \frac{1}{2}\rho +$$

$$\left.2\rho\ln\frac{m}{2E_e} + \frac{9}{4}\log\frac{\Lambda^2}{m^2} + K_v\right], \quad (10)$$

where m is the charged pion mass, λ is photon mass used as infrared regulator, Λ is ultraviolet (UV) cut off. In Eq. (10) we have defined

$$\rho = \ln\frac{2E_e}{m_e},$$

$$\beta = \sqrt{1 - \frac{4m^2}{s_\pi}}, \quad L_\beta = \ln\frac{1+\beta}{1-\beta},$$

$$\beta_\pm = \sqrt{1 - \frac{m^2}{E_\pm^2}}, \quad L_\pm = \ln\frac{1+\beta_\pm}{1-\beta_\pm}. \quad (11)$$

K_{v} depends on masses of particles and kinematics. Note that the UV-divergent part in Eq. (10) will cancel if the renormalized coupling $G_{\mathrm{F}}^2 V_{\mathrm{us}}^2$ is used instead of bare ones,
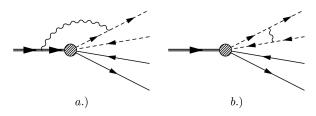

Fig. 7.   example vertex diagrams [14].

$$G_{\mathrm{F}}^2 V_{\mathrm{us}}^2 \to \left(1 - \frac{9}{4}\log\frac{\Lambda^2}{m^2}\right)\left(G_{\mathrm{F}}^2 V_{\mathrm{us}}^2\right)^{\mathrm{bare}}. \quad (12)$$

The soft photon contribution can be easily obtained, resulting in expression which is gauge invariant:

$$\frac{\mathrm{d}\Gamma_{\mathrm{soft}}}{\mathrm{d}\Gamma_{\mathrm{Born}}} = -\frac{\alpha}{4\pi^2}\int\frac{\mathrm{d}^3k}{\omega}\left(\frac{p}{pk} + \frac{q_-}{q_-k} - \frac{q_+}{q_+k} - \frac{p_e}{p_ek}\right)^2, \quad (13)$$

here k is photon momentum, ω is photon energy. It is straightforward to integrate out solid angle of photon momentum k and over its energy ω up to a limit $\omega < \Delta\epsilon$; we obtain:

$$\frac{\mathrm{d}\Gamma_{\mathrm{soft}}}{\mathrm{d}\Gamma_{\mathrm{Born}}} = \frac{\alpha}{\pi}\left[\ln\left(\frac{2\Delta\epsilon}{\lambda}\right)\left(-4 - \frac{L_-}{\beta_-} + \frac{L_+}{\beta_+} + \right.\right.$$

$$\left.2\rho + \frac{1+\beta^2}{\beta}L_\beta - 2\ln\frac{2p_e \cdot q_+}{2p_e \cdot q_-}\right) +$$

$$\rho - \rho^2 + K_s\right]. \quad (14)$$

Function K_{s} is dependent on masses of particles and kinematics. Soft singularity is again regularized with the photon mass λ.

The contribution of soft and virtual photons can be easily combined. It reads

$$\frac{\mathrm{d}\Gamma_{\mathrm{Born+virt+soft}}}{\mathrm{d}\Gamma_{\mathrm{Born}}} = 1 + \sigma P_\delta + \frac{\pi\alpha(1+\beta^2)}{2\beta} +$$

$$\frac{\alpha}{\pi}K_{\mathrm{vs}}, \quad (15)$$

where

$$P_\delta = 2\ln\frac{\Delta\epsilon}{E_e} + \frac{3}{2}, \quad \sigma = \frac{\alpha}{2\pi}(2\rho - 1), \qquad (16)$$

the expression of K_{vs} depends not only on masses of particles and kinematics, but also on soft photon energy cutoff $\Delta\epsilon$.

Staring from a certain energy threshold photons can be observed, at least in principle. Such contribution is called hard photon radiation and we will assume that it is defined by condition $\omega > \Delta\epsilon$. If soft photon matrix element Eq. (14) is used, and maximum energy of photon is taken from kinematical constraint E_e, then Eq. (14) can be used to calculate leading double logarithmic result of hard photon radiation. For that reason one need to subtract Eq. (14) calculated for E_e from that for $\Delta\epsilon$. Thus the contribution of hard photon emission by soft-photon-approximation is obtained,

$$\frac{d\Gamma_{Hard_{soft-like}}}{d\Gamma_{Born}} = \frac{\alpha}{\pi}\ln\left(\frac{\Delta\epsilon}{E_e}\right)\left(4 + \frac{L_-}{\beta_-} - \frac{L_+}{\beta_+} - 2\rho - \right.$$

$$\left. \frac{1+\beta^2}{\beta}L_\beta + 2\ln\frac{2p_e\cdot q_+}{2p_e\cdot q_-}\right). \qquad (17)$$

This result has to be corrected for single logarithm related to collinear photon emission along the charged outgoing decay products.

Photon emission from $e^\pm$ will give collinear singularity. Remaining charged products, π^+ and π^- are not relativistic. The electron part can be calculated with the help of collinear-photon-approximation. The squared collinear amplitude can be found in Ref. [15]. The actual formula for collinear contribution is taken from Ref. [16],

$$\frac{d\Gamma_{Collinear}}{d\Gamma_{Born}} = \frac{\alpha}{4\pi^2}\int\frac{d^3k}{\omega}\frac{z^2}{p_e\cdot k}\left(\frac{1+z^2}{1-z} - \frac{m_e^2}{p_e\cdot k}\right), \quad (18)$$

here

$$z = \frac{E_e}{E_e + \omega}.$$

First we integrate over solid angle of photon direction, later we integrate photon energy from $\Delta\epsilon$ to the maximum value E_e. Then the result of hard photon emitting from $e^\pm$ is obtained using collinear-photon-approximation,

$$\frac{d\Gamma_{Hard_e}}{d\Gamma_{Born}} = -\sigma P_\delta + \frac{\alpha}{2\pi}\left(3 - \frac{2}{3}\pi^2\right). \qquad (19)$$

Eq. (19) includes term proportional to $2\rho - 1$ which is already present in Eq. (17). This would lead to double counting. That is why we remove this term from

Eq. (17) and obtain

$$\frac{d\Gamma_{Hard_{no-e}}}{d\Gamma_{Born}} = \frac{\alpha}{\pi}\ln\left(\frac{\Delta\epsilon}{E_e}\right)\left(3 + \frac{L_-}{\beta_-} - \frac{L_+}{\beta_+} - \right.$$

$$\left. \frac{1+\beta^2}{\beta}L_\beta + 2\ln\frac{2p_e\cdot q_+}{2p_e\cdot q_-}\right). \qquad (20)$$

Finally hard (real) photon bremsstrahlung for photons of energy above $\Delta\epsilon$ reads

$$\frac{d\Gamma_{Hard}}{d\Gamma_{Born}} = \frac{d\Gamma_{Hard_e}}{d\Gamma_{Born}} + \frac{d\Gamma_{Hard_{no-e}}}{d\Gamma_{Born}}. \qquad (21)$$

If one adds real and virtual photons contribution together, one can obtain the expression as following,

$$\frac{d\Gamma_{Born+virt+real}}{d\Gamma_{Born}} = 1 + \frac{\pi\alpha(1+\beta^2)}{2\beta} + \frac{\alpha}{\pi}K. \qquad (22)$$

Complicated, but numerically small function K is dependent on masses of particles and kinematics of this process. Note that our final analytical result does not depend on the large logarithm

$$\ln\frac{2E_e}{m_e},$$

or soft photon energy cut $\Delta\epsilon$.

As one can see, Eqs. (15) (21), (22) are obtained with the help of approximations. Effectively it was assumed that matrix element at Born level can be always factorized out and photonic corrections can be calculated independently. Further corrections are assumed to be negligible and not affecting the substantial nature properties of hard interaction. This may be good as starting point, but cannot be left without future discussion/improvements[1].

Our formulas are based on the same scheme of calculation as explained in Ref. [14] and in principle they should coincide numerically. Some differences in analytical results are still present. Also some numerical results still remain different. The exact expressions for K_s, K_v, K_{vs} and K, as well as differences between our analytical results and these in Ref. [14] will not be listed here for the limit of paper length. They will be present elsewhere.

3.2 Numerical tests

Let's start with Eq. (22), the correction for distribution when photon is integrated out but all other kinematic variables are kept. In Figs. 8 and 9 we show that dominant part of Eq. (22) represents Coulomb correction. The difference is much smaller than the effect of Coulomb correction itself, see Fig. 10 where results for 1000 000 Born level events are placed in the histograms. We may conclude that our numer-

---

1)We are grateful to Prof. J. Gasser for stressing this point.

ical implementation of Eq. (22) works well since its dominant part represents Coulomb correction.
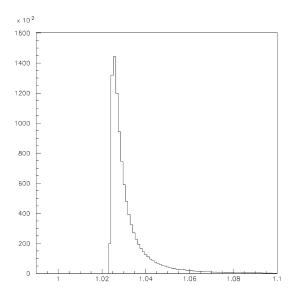

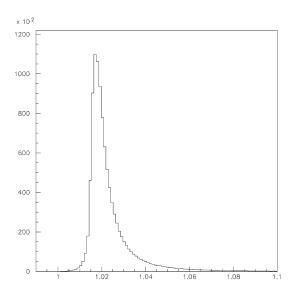
Fig. 8.   Coulomb correction from Ref. [10].

Fig. 9.   Radiative correction in Eq. (22).

We have done numerical tests with PHOTOS for soft photons and found the distribution of soft photons from PHOTOS is as same as given in the soft photon expression (Eq. (13)). We also have done the similar test using hard photon expression (Eq. (21)) and found it matches result from PHOTOS simulation in the soft photon region, too, as it is expected.

For harder photons, we compare result of PHOTOS, with results of Eq. (14) for soft photon and Eq. (21) for hard photon. Their ratios are given in Fig. 11, where effect as function of upper limit on photon energy was used. 100 000 000 PHOTOS event

samples were generated using single fixed Born level event.
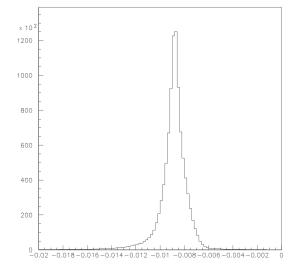

Fig. 10.   Difference between radiative correction in Eq. (22) and Coulomb correction from Ref. [10] calculated event by event.
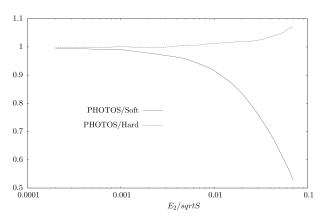

Fig. 11.   Ratios of result from PHOTOS to results using soft photon Eq. (14) and hard photon Eq. (21). Here $E_1 < E_\gamma < E_2$ where we set $\dfrac{E_2}{E_1} = 2.5$, E_2 varies from $0.0002\sqrt{S}$ to $0.07\sqrt{S}$. Note that the energy of electron $E_e \approx 0.07\sqrt{S}$.

We can conclude that agreement is good, as expected. Though differences especially in harder photon energy ranges can be seen. However even at the end of the spectrum, where distribution is poorly populated, differences are at 10 % level only.

4   Summary

We have presented the new tests of PHOTOS Monte Carlo, where the exact matrix element of

$\gamma^* \to \pi^+\pi^-\gamma$ is implemented and its numerical result is compared with the kernel of PHOTOS. QED radiative correction to process $K^\pm \to l^\pm\nu\pi^+\pi^-(\gamma)$ is also studied analytically. Reasonable numerical agreement with simulations including Coulomb correction and PHOTOS Monte Carlo was found. Since several assumptions are employed, further work is necessary. Our result is of practical interest for experiments. They confirm that at least on technical level the Monte Carlo program works well as expected.

References

1 Barberio E, van Eijk B, Was Z. Comput. Phys. Commun., 1991, **66**: 115–128
2 Barberio E, Was Z. Comput. Phys. Commun., 1994, **79**: 291–308
3 Jadach S, Ward B F L, Was Z. Phys. Rev. D, 2001, **63**: 113009
4 Jadach S, Ward B F L, Was Z. Comput. Phys. Commun., 2000, **130**: 260–325
5 Golonka P, Was Z. Eur. Phys. J. C, 2007, **50**: 53–62
6 Andonov A et al. Acta Phys. Polon. B, 2003, **34**: 2665–2672
7 Nanava G, Was Z. Eur. Phys. J. C, 2007, **51**: 569–583
8 Nanava G, Was Z. Acta Phys. Polon, 2003, **B34**: 4561–4570
9 Nanava G, Xu Q, Was Z. arXiv: 0906.4052 [hep-ph]
10 NA48/2, Batley J R et al. Eur. Phys. J. C, 2008, **54**: 411–423
11 Colangelo G, Gasser J, Leutwyler H. Nucl. Phys. B, 2001, **603**: 125–179; hep-ph/0103088
12 Czyz H et al. Eur. Phys. J. C, 2003, **27**: 563–575
13 Jadach S, Ward B F L, Was Z. Phys. Lett. B, 1999, **449**: 97–108
14 Bystritskiy Yu M, Gevorkyan S R, Kuraev E A. Eur. Phys. J. C, 2009, **64**: 47–54, arXiv: 0906.0516 [hep-ph]
15 Baier V N, Fadin V S, Khoze V A. Nucl. Phys. B, 1973, **65**: 381–396
16 XU Qing-Jun. ph.D. thesis, 2006, Technical University of Munich, Germany, arXiv: 0912.5160 [hep-ph]